Journal of Nuclear Medicine, published on January 15, 2021 as doi:10.2967/jnumed.120.259226

Detection of Early Progression with ^{18}F-DCFPyL PET/CT in Men with Metastatic Castration-Resistant Prostate Cancer Receiving Bipolar Androgen Therapy

Mark C. Markowski[1*], Pedro Isaacsson Velho[1,2], Mario A. Eisenberger[1], Martin G. Pomper[1,3], Kenneth J. Pienta[4], Michael A. Gorin[4], Emmanuel S. Antonarakis[1], Samuel R. Denmeade[1], Steven P. Rowe[1,3]

[1] Department of Oncology, Sidney Kimmel Comprehensive Cancer Center at Johns Hopkins, Baltimore, MD
[2] Department of Medical Oncology, Hospital Moinhos de Vento, Porto Alegre, Brazil
[3] The Russel H. Morgan Department of Radiology and Radiological Science, Johns Hopkins University School of Medicine, Baltimore, MD
[4] The James Buchanan Brady Urological Institute and Department of Urology, Johns Hopkins University School of Medicine, Baltimore, MD

***CORRESPONDING AUTHOR**

Mark C. Markowski, M.D. Ph.D.
Johns Hopkins Medical Institutions
Sidney Kimmel Cancer Center
Viragh Building, 9th floor
201 N Broadway
Baltimore, MD 21287
Email: mmarko12@jhmi.edu

RUNNING TITLE
PSMA PET Detects Progression on BAT

ACKNOWLEDGEMENTS
The project described was supported by the Sidney Kimmel Comprehensive Cancer Center at Johns Hopkins NIH grant P30 CA006973, R01 CA184012, Patrick C. Walsh, PCF Challenge and Young Investigator Awards. The content is solely the responsibility of the authors and does not necessarily represent the official views of the National Cancer Institute or the National Institutes of Health.

ABSTRACT

Rationale: Bipolar androgen therapy (BAT) is an emerging treatment for metastatic castration resistant prostate cancer (mCRPC). ^{18}F-DCFPyL is a small-molecule positron emission tomography (PET) radiotracer targeting prostate-specific membrane antigen (PSMA). We analyzed the utility of ^{18}F-DCFPyL PET/CT in determining clinical response to BAT.

Methods: Six men with mCRPC receiving BAT were imaged with ^{18}F-DCFPyL PET/CT at baseline and after 3 months of treatment. Progression by PSMA-targeted PET/CT was defined as the appearance of any new ^{18}F-DCFPyL-avid lesion.

Results: Three of 6 (50%) patients had progression on ^{18}F-DCFPyL PET/CT. All three had stable disease or better on contemporaneous conventional imaging. Radiographic progression on CT and/or bone scan was observed within 3 months of progression on ^{18}F-DCFPyL PET/CT. For the 3 patients that did not have progression on ^{18}F-DCFPyL PET/CT, radiographic progression was not observed for $\geq$ 6 months.

Conclusions: New radiotracer-avid lesions on ^{18}F-DCFPyL PET/CT in men with mCRPC undergoing BAT can indicate early progression.

KEY WORDS

PSMA, Testosterone, Early progression

INTRODUCTION

The imaging of prostate cancer (PCa) in many parts of the world has recently been revolutionized by the introduction of small-molecule positron emission tomography (PET) radiotracers that bind to prostate-specific membrane antigen (PSMA)(*1*). PSMA is a transmembrane glycoprotein that is expressed in a large majority of prostate cancers (*2*). Those agents, which include both ^{68}Ga-labeled (e.g. ^{68}Ga-PSMA-11(*3*)) and ^{18}F-labeled (e.g. ^{18}F-DCFPyL(*4*)) compounds, have been shown to have high rates of detection of sites of PCa in a variety of disease states (*5*).

There is an interplay between androgen signaling and PSMA expression in which blockade of the androgen-signaling pathway leads to upregulation of PSMA (*6*). Varying responses to androgen-axis-targeted therapies have been observed on serial PSMA-targeted PET studies (*7*), making it difficult to assess response to such therapies. To date, changes in serial PSMA-targeted PET have not been described in the context of bipolar androgen therapy (BAT).

BAT is being tested as a novel treatment for men with metastatic castration resistant PCa (mCRPC). Testosterone is administered to supraphysiologic circulating levels, which subsequently decrease over a 28-day cycle back to near-castrate levels (*8*). All men are maintained on androgen deprivation to suppress endogenous testosterone production from the testes. Several studies have demonstrated efficacy of BAT as a treatment option for mCRPC patients (*9-11*). Measuring the clinical benefit of BAT using changes in prostate-specific antigen (PSA) is difficult since radiographic regression of disease has been observed with stable or rising PSA values (*10,11*).

A novel imaging strategy to determine patients at high risk of progression on BAT is needed. In this pilot study, we examined changes in ^{18}F-DCFPyL PET imaging following treatment with BAT in men with mCRPC.

METHODS

^{18}F-DCFPyL PET/CT imaging was obtained as part of an Institutional Review Board-approved, prospective sub-study on two clinical trials for men initiating treatment with BAT (ClinicalTrials.gov identifiers NCT02286921 and NCT03554317). Written informed consent was obtained on all participants. All participants had mCRPC and prior treatment with at least one novel AR-targeted therapy. PET/CT images were acquired on either a Siemens Biograph mCT 128-slice (Siemens Healthineers, Erlangen, Germany) or a GE Discovery RX 64-slice (GE Healthcare, Waukesha, WI, USA) scanner utilizing 3D emission mode with CT-based attenuation correction. Scans were initiated 60 minutes after the intravenous infusion of 333 MBq (9 mCi) of ^{18}F-DCFPyL with a field-of-view from the mid-thighs through the skull vertex. Images were reconstructed with a standard ordered-subset expectation maximization method.

All ^{18}F-DCFPyL PET/CT scans were interpreted by a single radiologist (S. P. Rowe) who was blinded to the details of the patient's disease status while on BAT. Radiotracer uptake outside of the normal biodistribution of ^{18}F-DCFPyL was categorized according to the PSMA-RADS version 1.0 interpretive framework and lesions that were PSMA-RADS-3A/3B/4/5 were considered positive for PCa (*12*). Maximum standardized uptake values (SUV_{max}) were recorded for all lesions on

baseline and follow-up scans (Supplemental Table 1). According to the study protocol, patients underwent ^{18}F-DCFPyL PET/CT imaging prior to starting, and after 3 cycles, of BAT. Clinicians were blinded to the results of ^{18}F-DCFPyL PET/CT imaging and those results were not used in clinical management.

Comparisons were made between the pre- and on-treatment PSMA-targeted PET/CT imaging to determine progression. PSMA progression was defined as having one or more new lesions deemed by the interpreting radiologist to be consistent with radiotracer-avid PCa. Radiographic progression on conventional imaging was defined by RECIST 1.1 (soft tissue lesions) and PCWG3 (clinical and bone lesions) guidelines, and objective response was defined using RECIST 1.1 (*13,14*).

RESULTS

Six patients were enrolled. Five of six (83.3%) began BAT on the same day as their baseline ^{18}F-DCFPyL PET, while the final patient started BAT the following day. From initiation of therapy to follow-up PET was a median of 84 days (interquartile range, 83.25 – 87.75). At the time of the follow-up PET, repeat imaging was obtained with CT and bone scan.

Best PSA and change in tumor response are listed for each patient (Table 1). Four of six (66.7%) patients had a PSA_{50} response and one patient achieved an objective response on conventional imaging. We assessed each patient for progression on PSMA-targeted imaging as described above. Three of six (50.0%) patients had progression on ^{18}F-DCFPyL PET/CT. A description of each ^{18}F-DCFPyL PET/CT lesion is provided (Supplemental Table 1). None of the patients had evidence of radiographic progression on conventional imaging at the time of the

follow-up ^{18}F-DCFPyL PET/CT. Two patients that achieved a PSA_{50} response with stable disease on CT and bone scan had new lesions seen on ^{18}F-DCFPyL PET. Neither patient with a PSA_{90} response had progression on ^{18}F-DCFPyL PET/CT. Maximum intensity projections of the ^{18}F-DCFPyL PET/CT for patients pre- and on-treatment are shown (Figure 1). Many radiotracer-avid lesions reduced in intensity following BAT. For instance, Patient #1 had a complete PSMA response to BAT (i.e. 100% reduction in SUV_{max} across all PSMA avid lesions) in the clinical context of a rising PSA on therapy. Patients #4-6 had at least one new PSMA-avid lesion that developed on BAT. In all three cases of progression on PET/CT, the majority of ^{18}F-DCFPyL avid lesions decreased in intensity.

We next explored the relationship between ^{18}F-DCFPyL PET/CT findings and radiographic progression on conventional imaging. In the three patients that did not have progression on ^{18}F-DCFPyL PET/CT, radiographic progression on BAT was not observed until 6-9 months following the second PET/CT (Figure 2). In contrast, all patients with progression on PET/CT had evidence of progression on conventional imaging by 3 months. In all instances of early progression, the sites of progression on CT or bone scan correlated with the PSMA-targeted PET findings.

DISCUSSION

BAT and PSMA-targeted imaging both remain under clinical investigation for patients with PCa. When testosterone binds to AR, it induces PSA expression, meaning there is an urgent need for the development of a biomarker that can identify early disease progression since rising PSA is unreliable.

We performed a pilot imaging study assessing the effect of BAT on ^{18}F-DCFPyL PET/CT imaging. Following initiation of treatment, most sites of radiotracer uptake had a decrease in SUV_{max} at the 3-month time point. There are several possible explanations for this finding. One is that BAT induced regression of disease across multiple sites, which is consistent with the lack of radiographic progression after three months of therapy. However, given the degree of change in SUV_{max}, one would expect to see more objective responses at that time point. A second explanation is that BAT inhibits the expression of PSMA protein. Prior studies have shown that AR inhibition increases PSMA expression and may cause "flare" on PSMA-targeted PET (*6,15*). It is plausible that reengagement of AR via exogenous testosterone may downregulate PSMA expression while maintaining tumor viability. This artifact would result in a false negative scan. Alternatively, BAT may downregulate PSMA protein as an early event to apoptosis. It has been shown that PSMA may direct cellular growth through PI3K-AKT signaling (*16*). Thus, decreasing PSMA expression may result in tumor regression. True radiographic progression did not occur for 9-12 months after the ^{18}F-DCFPyL PET scan, which would support these findings being indicative of an early clinical response. Arguing against transcriptional inhibition of PMSA expression are the findings of new or worsening ^{18}F-DCFPyL avid lesions. That phenomenon was only observed in patients who experienced radiographic progression at their next restaging scan.

The utility of ^{18}F-DCFPyL PET/CT imaging may be in identifying those patients at highest risk of progressing on BAT. Patients that demonstrate new ^{18}F-DCFPyL-avid lesions all had early radiographic progression.

This study was limited by the small number of patients and only two imaging time points. In addition, all scans were read by a single radiologist who, although blinded, could bias the results of the study. A larger prospective study is underway to confirm these findings (NCT04424654).

CONCLUSION

Treatment with BAT induced radiographic changes on ^{18}F-DCFPyL PET/CT imaging. New radiotracer-avid lesions on ^{18}F-DCFPyL PET/CT in men with mCRPC undergoing BAT can indicate early progression.

CONFLICT OF INTEREST

M.G.P. is a co-inventor on a U.S. patent covering ^{18}F-DCFPyL and as such is entitled to a portion of any licensing fees and royalties generated by this technology. This arrangement has been reviewed and approved by the Johns Hopkins University in accordance with its conflict-of-interest policies. S.P.R. is a consultant to Progenics Pharmaceuticals, the licensee of ^{18}F-DCFPyL. M.A.G. has served as a consultant to Progenics Pharmaceuticals. M.G.P., K.J.P., M.A.G., and S.P.R. receive research funding from Progenics Pharmaceuticals.

KEY POINTS

Question: Early progression on BAT is difficult to detect given the effect of testosterone on PSA expression and limitations of conventional imaging.

Pertinent Findings: New radiotracer-avid lesions on ^{18}F-DCFPyL PET/CT imaging were observed in mCRPC patients on BAT who experienced early conventional radiographic progression.

Implications for Patient Care: PSMA-targeted PET/CT may identify mCRPC patients at risk of early progression on BAT.

FIGURES AND FIGURE LEGENDS

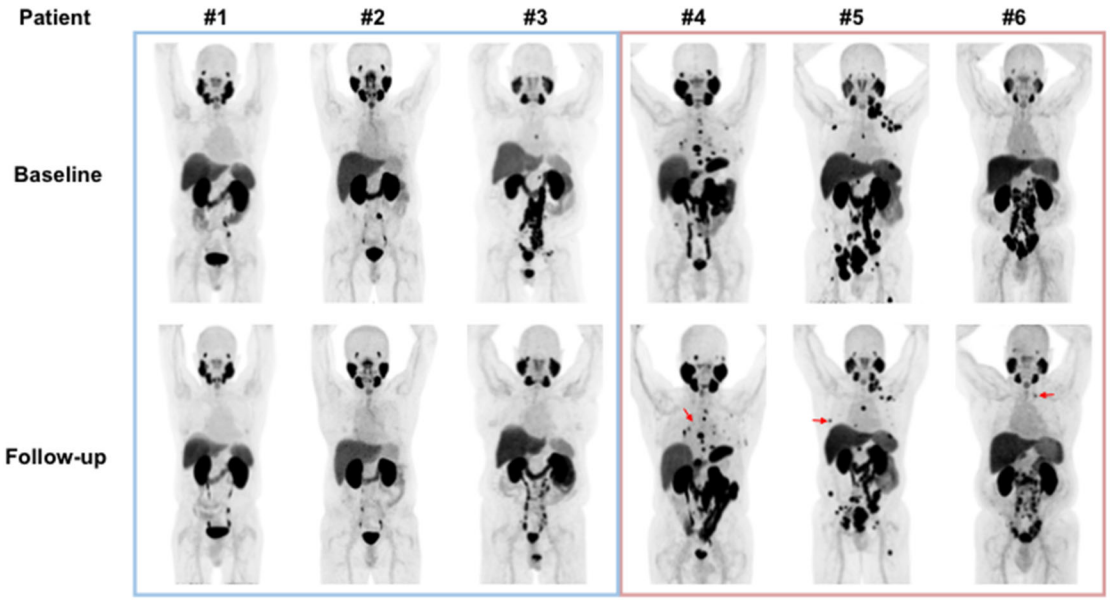

Figure 1: Changes in ^{18}F-DCFPyL PET/CT imaging Following 3 Months of BAT.

Baseline (top row) and follow-up (bottom row) maximum intensity projection (MIP) whole-body images for each of the patients included in this study. For patients #4-#6, representative new lesions/sites of progression are demarcated with red arrows. Additional new lesions may be hidden by normal uptake or other sites of disease.

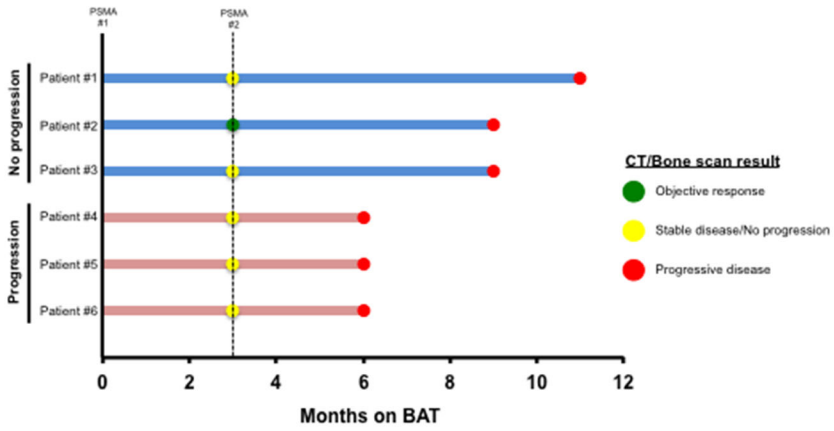

Figure 2: Swimmers Plot Showing Radiographic Response/Progression on BAT

All patients were followed until radiographic progression. ^{18}F-DCFPyL PET/CT imaging was obtained prior to the start of bipolar androgen therapy and after 3 months of treatment. Patients #1-3 (blue lines) had no progression noted with ^{18}F-DCFPyL. Patients #4-6 (red lines) had new ^{18}F-DCFPyL-avid lesions. These data suggest that disease progression on PSMA-targeted PET imaging precedes detection on conventional imaging.

TABLE AND TABLE LEGEND

Patient	PSA Change	Tumor Change	PSMA Result
1	93%	NE	No Progression
2	-98%	-44%	No Progression
3	-93%	-23%	No Progression
4	1%	-11%	Progression
5	-55%	-2%	Progression
6	-63%	-25%	Progression

Table 1: Table 1. Best Biochemical, Radiographic, and ^{18}F-DCFPyL Response After 3 Months of BAT (NE = Not Evaluable).

REFERENCES

1. Rowe SP, Gorin MA, Pomper MG. Imaging of prostate-specific membrane antigen with small-molecule PET radiotracers: From the bench to advanced clinical applications. *Annu Rev Med.* 2019;70:461-477.

2. Wright GL, Jr., Haley C, Beckett ML, Schellhammer PF. Expression of prostate-specific membrane antigen in normal, benign, and malignant prostate tissues. *Urol Oncol.* 1995;1:18-28.

3. Afshar-Oromieh A, Malcher A, Eder M, et al. PET imaging with a [68Ga]gallium-labelled PSMA ligand for the diagnosis of prostate cancer: biodistribution in humans and first evaluation of tumour lesions. *Eur J Nucl Med Mol Imaging.* 2013;40:486-495.

4. Szabo Z, Mena E, Rowe SP, et al. Initial evaluation of [(18)F]DCFPyL for prostate-specific membrane antigen (PSMA)-targeted PET imaging of prostate cancer. *Mol Imaging Biol.* 2015;17:565-574.

5. Perera M, Papa N, Christidis D, et al. Sensitivity, specificity, and predictors of positive (68)Ga-prostate-specific membrane antigen positron emission tomography in advanced prostate cancer: A systematic review and meta-analysis. *Eur Urol.* 2016;70:926-937.

6. Evans MJ, Smith-Jones PM, Wongvipat J, et al. Noninvasive measurement of androgen receptor signaling with a positron-emitting radiopharmaceutical that targets prostate-specific membrane antigen. *Proc Natl Acad Sci U S A.* 2011;108:9578-9582.

7. Aggarwal R, Wei X, Kim W, et al. Heterogeneous flare in prostate-specific membrane antigen positron emission tomography tracer uptake with initiation of androgen pathway blockade in metastatic prostate cancer. *Eur Urol Oncol.* 2018;1:78-82.

8. Denmeade SR, Isaacs JT. Bipolar androgen therapy: the rationale for rapid cycling of supraphysiologic androgen/ablation in men with castration resistant prostate cancer. *Prostate.* 2010;70:1600-1607.

9. Schweizer MT, Wang H, Luber B, et al. Bipolar androgen therapy for men with androgen ablation naive prostate cancer: Results from the Phase II BATMAN Study. *Prostate.* 2016;76:1218-1226.

10. Teply BA, Wang H, Luber B, et al. Bipolar androgen therapy in men with metastatic castration-resistant prostate cancer after progression on enzalutamide: an open-label, phase 2, multicohort study. *Lancet Oncol.* 2018;19:76-86.

11. Markowski MC, Wang H, Sullivan R, et al. A multicohort open-label Phase II trial of bipolar androgen therapy in men with metastatic sastration-resistant prostate cancer (RESTORE): A comparison of post-abiraterone versus post-enzalutamide cohorts. *Eur Urol.* 2020; Epub ahead of print.

12. Rowe SP, Pienta KJ, Pomper MG, Gorin MA. PSMA-RADS Version 1.0: A step towards standardizing the interpretation and reporting of PSMA-targeted PET imaging studies. *Eur Urol.* 2018;73:485-487.

13. Eisenhauer EA, Therasse P, Bogaerts J, et al. New response evaluation criteria in solid tumours: revised RECIST guideline (version 1.1). *Eur J Cancer.* 2009;45:228-247.

14. Scher HI, Morris MJ, Stadler WM, et al. Trial design and objectives for castration-resistant prostate cancer: Updated recommendations from the prostate cancer clinical trials working group 3. *J Clin Oncol.* 2016;34:1402-1418.

15. Hope TA, Truillet C, Ehman EC, et al. 68Ga-PSMA-11 PET Imaging of response to androgen receptor inhibition: First human experience. *J Nucl Med.* 2017;58:81-84.

16. Caromile LA, Shapiro LH. PSMA redirects MAPK to PI3K-AKT signaling to promote prostate cancer progression. *Mol Cell Oncol.* 2017;4:e1321168.

	Scan #1	Lesions	SUVmax	Size	Scan #2	Lesions	SUVmax	Size	DeltaSUVAbsolute	DeltaSUV%
Patient #1		Left para-aortic LN	3.9	0.4		Left para-aortic LN	N/A	0.4	-3.9	-100
		Left para-aortic LN	11.4	0.3		Left para-aortic LN	N/A	0.3	-11.4	-100
		Left prostate	20.2	N/A		Left prostate	N/A	N/A	-20.2	-100
		Rightprostate	9.9	N/A		Right prostate	N/A	N/A	-9.9	-100
Patient #2		Left common iliac LN	16.0	1.9		Left common iliac LN	3.1	0.8	-12.9	-80.625
Patient #3		Paraesophageal LN	11.8	0.3		Paraesophageal LN	N/A	N/A	-11.8	-100
		Left para-aortic LN	42.8	0.6		Left para-aortic LN	N/A	0.2	-42.8	-100
		Left para-aortic LN	50.9	0.5		Left para-aortic LN	5.7	0.3	-45.2	-88.80157171
		Left para-aortic LN	46.3	0.3		Left para-aortic LN	N/A	0.3	-46.3	-100
		Left para-aortic LN	65.2	0.6		Left para-aortic LN	9.2	0.4	-56	-85.88957055
		Aortocaval LN	61.5	0.5		Aortocaval LN	N/A	0.2	-61.5	-100
		Left para-aortic LN	35.0	0.4		Left para-aortic LN	N/A	0.2	-35.0	-100
		Left para-aortic LN	40.8	0.3		Left para-aortic LN	9.9	0.3	-30.9	-75.73529412
		Aortocaval LN	37.6	0.3		Aortocaval LN	3.9	0.2	-33.7	-89.62765957
		Retrocaval LN	36.9	0.6		Retrocaval LN	11.8	0.4	-25.1	-68.02168022
		L3	46.5	N/A		L3	N/A	N/A	-46.5	-100
		Right common iliac LN	53.9	0.5		Right common iliac LN	N/A	N/A	-53.9	-100
		Left common iliac LN	52.3	0.5		Left common iliac LN	N/A	0.2	-52.3	-100
		Right common iliac LN	57.2	0.5		Right common iliac LN	N/A	0.2	-57.2	-100
		Aortic bifurcation LN	25.9	0.3		Aortic bifurcation LN	N/A	N/A	-25.9	-100
		Left common iliac LN	57.4	0.9		Left common iliac LN	16.2	0.6	-41.2	-71.77700348
		Left internal iliac LN	21.7	0.3		Left internal iliac LN	N/A	N/A	-21.7	-100
		Right external iliac LN	5.4	0.3		Right external iliac LN	5.5	0.3	0.1	1.851851852
		Left external iliac LN	8.0	0.5		Left external iliac LN	6.2	0.5	-1.8	-22.5
		Left external iliac LN	49.8	0.6		Left external iliac LN	8.1	0.4	-41.7	-83.73493976
		Left external iliac LN	30.4	0.3		Left external iliac LN	N/A	N/A	-30.4	-100
		Left internal iliac LN	16.3	0.3		Left internal iliac LN	N/A	N/A	-16.3	-100
		Right seminal vesicle	18.1	N/A		Right seminal vesicle	N/A	N/A	-18.1	-100
		Left sciatic nerve implant	13.1	N/A		Left sciatic nerve implant	N/A	N/A	-13.1	-100
Patient #4		C4	2.1	N/A		C4	N/A	N/A	-3.9	-100
		C4	2.4	N/A		C4	N/A	N/A	-3.9	-100
		C5	1.3	N/A		C5	1.8	N/A	0.5	38.46153846
		C6	1.6	N/A		C6	N/A	N/A	-3.0	-100
		C6	1.3	N/A		C6	N/A	N/A	-2.4	-100
		T2 transverse process	3.6	N/A		T2 transverse process	2.2	N/A	-1.4	-38.88888889
		T3	6.0	N/A		T3	2.0	N/A	-4.0	-66.66666667
		T3	3.2	N/A		T3	2.1	N/A	-1.1	-34.375
		Manubrium	5.3	N/A		Manubrium	7.4	N/A	2.1	39.62264151
		Left rib #2	2.4	N/A		Left rib #2	1.4	N/A	-1	-41.66666667
		Left rib #2	5.2	N/A		Left rib #2	3.9	N/A	-1.3	-25
		Left scapula	0.8	N/A		Left scapula	N/A	N/A	0.8	-100

	T4	18.3	N/A	T4	12.4	N/A	-5.9	-32.24043716
	T5	4.8	N/A	T5	3.0	N/A	-1.8	-37.5
	T5	3.2	N/A	T5	2.2	N/A	-1	-31.25
	Left rib #5	2.3	N/A	Left rib #5	3.3	N/A	1	43.47826087
	Left hilum LN	4.0	0.5	Left hilum LN	4.0	0.5	0	0
	Right hilum LN	9.3	0.5	Right hilum LN	5.5	0.5	-3.8	-40.86021505
	Right rib #5	N/A	N/A	Right rib #5	2.9	N/A	2.9	100
	T5	N/A	N/A	T5	3.7	N/A	3.7	100
	Right hilum LN	9.3	0.5	Right hilum LN	8.9	0.8	-0.4	-4.301075269
	Left hilum LN	5.3	0.6	Left hilum LN	5.2	0.6	-0.1	-1.886792453
	T7	27.5	N/A	T7	14.4	N/A	-13.1	-47.63636364
	T7	23.4	N/A	T7	10.4	N/A	-13	-55.55555556
	Left rib #7	10.9	N/A	Left rib #7	1.8	N/A	-9.1	-83.48623853
	Left rib #3	3.9	N/A	Left rib #3	2.4	N/A	-1.5	-38.46153846
	Sternum	5.9	N/A	Sternum	2.8	N/A	-3.1	-52.54237288
	T9	27	N/A	T9	10.9	N/A	-16.1	-59.62962963
	Left rib #9	14.8	N/A	Left rib #9	11.0	N/A	-3.8	-25.67567568
	T11	49.0	N/A	T11	24.6	N/A	-24.4	-49.79591837
	Aortocaval LN	24.2	0.8	Aortocaval LN	8.1	0.6	-16.1	-66.52892562
	Left para-aortic LN	84.2	1.7	Left para-aortic LN	43.7	1.7	-40.5	-48.09976247
	Aortocaval LN	21.4	0.6	Aortocaval LN	12.4	0.6	-9	-42.05607477
	Right common iliac LN	7.7	0.4	Right common iliac LN	5.9	0.4	-1.8	-23.37662338
	Right iliac	6.7	N/A	Right iliac	3.5	N/A	-3.2	-47.76119403
	Right iliac	2.8	N/A	Right iliac	4.0	N/A	1.2	42.85714286
	Sacrum	13.2	N/A	Sacrum	3.0	N/A	-10.2	-77.27272727
	Sacrum	5.1	N/A	Sacrum	5.4	N/A	0.3	5.882352941
Patient #5	Left supraclavicular LN	20.2	1.2	Left supraclavicular LN	11.2	1.1	-9	-44.55445545
	Left supraclavicular LN	15.8	0.8	Left supraclavicular LN	11.6	0.4	-4.2	-26.58227848
	Left supraclavicular LN	9.2	0.4	Left supraclavicular LN	N/A	N/A	-9.2	-100
	Left supraclavicular LN	13.6	1.0	Left supraclavicular LN	11.7	0.5	-1.9	-13.97058824
	Left supraclavicular LN	11.2	0.6	Left supraclavicular LN	N/A	N/A	-11.2	-100
	Left supraclavicular LN	N/A	N/A	Left supraclavicular LN	6.2	0.4	6.2	100
	Left axillary LN	13.9	0.6	Left axillary LN	N/A	N/A	-13.9	-100
	Left axillary LN	13.0	0.6	Left axillary LN	9.8	0.6	-3.2	-24.61538462
	Left scapula	8.2	N/A	Left scapula	17.8	N/A	9.6	117.0731707
	Left axillary LN	12.9	0.8	Left axillary LN	2.7	0.4	-10.2	-79.06976744
	Left axillary LN	11.6	1.2	Left axillary LN	4.9	0.5	-6.7	-57.75862069
	Left axillary LN	11.8	1.0	Left axillary LN	1.9	0.4	-9.9	-83.89830508
	Rigth rib #4	20.9	N/A	Right rib #4	N/A	N/A	-20.9	-100
	Sternum	13.0	N/A	Sternum	22.5	N/A	9.5	73.07692308
	T5	6.2	N/A	T5	N/A	N/A	-6.2	-100
	Right rib #7	N/A	N/A	Right rib #7	10.3	N/A	10.3	100

	Right rib #9	18.3	N/A	Right rib #9	7.9	N/A	-10.4	-56.83060109
	Left rib #9	40.7	N/A	Left rib #9	18.5	N/A	-22.2	-54.54545455
	T11	N/A	N/A	T11	12.9	N/A	12.9	100
	Retrocrural LN	6.9	0.3	Retrocrural LN	3.4	0.2	-3.5	-50.72463768
	Retrocrural LN	6.6	0.2	Retrocrural LN	3.1	0.2	-3.5	-53.03030303
	Retrocrural LN	9.8	0.3	Retrocrural LN	6.0	0.3	-3.8	-38.7755102
	T12	20.2	N/A	T12	30.7	N/A	10.5	51.98019802
	Left peri-aortic LN	12.2	0.8	Left peri-aortic LN	8.8	0.4	-3.4	-27.86885246
	Left peri-aortic LN	12.5	0.6	Left peri-aortic LN	N/A	0.3	-12.5	-100
	Retrocaval LN	9.6	1.2	Retrocaval LN	11.4	0.8	1.8	18.75
	L1	N/A	N/A	L1	7.7	N/A	7.7	100
	Left peri-aortic LN	16.5	1.6	Left peri-aortic LN	13.4	0.6	-3.1	-18.78787879
	Left peri-aortic LN	16.5	1.2	Left peri-aortic LN	13.3	1.1	-3.2	-19.39393939
	L1	6.3	N/A	L2	30.5	N/A	24.2	384.1269841
	Precaval LN	8.4	0.7	Precaval LN	8.6	0.7	0.2	2.380952381
	Retrocaval LN	15.9	1.0	Retrocaval LN	2.9	0.4	-13	-81.76100629
	Left peri-aortic LN	18.8	1.2	Left peri-aortic LN	16.2	1.2	-2.6	-13.82978723
	Left iliac	73.7	N/A	Left iliac	32.9	N/A	-40.8	-55.35956581
	Right iliac	7.5	N/A	Right iliac	35.0	N/A	27.5	366.6666667
	Left common iliac LN	22.1	1.2	Left common iliac LN	14.2	1.2	-7.9	-35.74660633
	Sacrum	55.9	N/A	Sacrum	28.4	N/A	-27.5	-49.19499106
	Sacrum	17.2	N/A	Sacrum	28.2	N/A	11	63.95348837
	Left external iliac LN	20.1	1.8	Left external iliac LN	20.5	1.8	0.4	1.990049751
	Right external iliac LN	22.1	1.5	Right external iliac LN	13.8	0.6	-8.3	-37.55656109
	Right iliac	N/A	N/A	Right iliac	14.8	N/A	14.8	100
	Sacrum	85.7	N/A	Sacrum	27.3	N/A	-58.4	-68.14469078
	Right iliac	36.8	N/A	Right iliac	41.6	N/A	4.8	13.04347826
	Left sciatic nerve implant	29.9	N/A	Left sciatic nerve implant	16.3	N/A	-13.6	-45.48494983
	Left inguinal LN	7.9	0.3	Left inguinal LN	9.0	0.3	1.1	13.92405063
	Right femur	8.8	N/A	Right femur	1.3	N/A	-7.5	-85.22727273
	Left thigh	21.4	N/A	Left thigh	20.9	N/A	-0.5	-2.336448598
Patient #6	Left supraclavicular LN	N/A	N/A	Left supraclavicular LN	6.5	0.5	6.5	100
	Paraesophageal LN	7.3	0.4	Paraesophageal LN	3.0	0.4	-4.3	-58.90410959
	Left retrucrual LN	10.9	0.3	Left retrocrural LN	2.0	0.3	-8.9	-81.65137615
	Retrocaval LN	17.1	1.0	Retrocaval LN	11.9	1.2	-5.2	-30.40935673
	Precaval LN	N/A	N/A	Precaval LN	8.6	0.6	8.6	100
	Left peri-aortic LN	7.5	0.8	Left peri-aortic LN	4.4	1.2	-3.1	-41.33333333
	Left peri-aortic LN	N/A	N/A	Left peri-aortic LN	5.9	0.6	5.9	100
	Pre-aortic LN	8.3	1.2	Pre-aortic LN	12.6	1.6	4.3	51.80722892
	Left peri-aortic LN	23.8	1.6	Left peri-aortic LN	6.1	0.7	-17.7	-74.3697479
	Left peri-aortic LN	14.9	1.8	Left peri-aortic LN	6.3	0.6	-8.6	-57.71812081
	Precaval LN	12.9	0.6	Precaval LN	12.1	0.8	-0.8	-6.201550388

	Left peri-aortic LN	14.8	1.5	Left peri-aortic LN	8.8	1.5	-6	-40.54054054
	Right common iliac LN	13.9	1.2	Right common iliac LN	10.9	0.9	-3	-21.58273381
	Right common iliac LN	10.8	1.0	Right common iliac LN	8.9	0.8	-1.9	-17.59259259
	Aortic bifurcation LN	9.4	1.1	Aortic bifurcation LN	5.0	0.8	-4.4	-46.80851064
	Aortic bifurcation LN	19.2	1.3	Aortic bifurcation LN	N/A	0.8	-19.2	-100
	Left common iliac LN	9.6	1.1	Left common iliac LN	5.6	0.9	-4	-41.66666667
	Left common iliac LN	27.9	1.4	Left common iliac LN	7.9	0.8	-20	-71.68458781
	Right external iliac LN	25.9	1.0	Right external iliac LN	4.1	0.6	-21.8	-84.16988417
	Presacral LN	18.4	1.2	Presacral LN	8.2	0.9	-10.2	-55.43478261
	Presacral LN	7.6	0.8	Presacral LN	7.2	0.8	-0.4	-5.263157895
	Right external iliac LN	55.3	2.5	Right external iliac LN	5.3	1.1	-50	-90.4159132
	Right external iliac LN	21.4	1.1	Right external iliac LN	N/A	0.8	-21.4	-100
	Left external iliac LN	13.1	3.1	Left external iliac LN	11.9	2.4	-1.2	-9.160305344
	Left external iliac LN	17.4	2.7	Left external iliac LN	9.2	1.1	-8.2	-47.12643678
	Left external iliac LN	25.2	2.9	Left external iliac LN	7.3	0.9	-17.9	-71.03174603
	Right external iliac LN	50.8	2.7	Right external iliac LN	8.7	2.1	-42.1	-82.87401575
	Left external iliac LN	13.4	3.1	Left external iliac LN	10.2	2.4	-3.2	-23.88059701
	Prostate	22.5	N/A	Prostate	3.9	N/A	-18.6	-82.66666667